Current Resonances in Graphene with Time-Dependent Potential Barriers

Sergey E. Savel'ev,[1] Wolfgang Häusler,[2] and Peter Hänggi[2]
[1]Department of Physics, Loughborough University, Loughborough LE11 3TU, United Kingdom
[2]Institut für Physik, Universität Augsburg, D-86135 Augsburg, Germany
(Received 25 July 2011; published 30 November 2012)

A method is derived to solve the massless Dirac-Weyl equation describing electron transport in a monolayer of graphene with a scalar potential barrier $U(x, t)$, homogeneous in the y direction, of arbitrary space and time dependence. Resonant enhancement of both electron backscattering and currents, across and along the barrier, is predicted when the modulation frequencies satisfy certain resonance conditions. These conditions resemble those for Shapiro steps of driven Josephson junctions. Surprisingly, we find a nonzero y component of the current for carriers of zero momentum along the y-axis.

DOI: 10.1103/PhysRevLett.109.226602 PACS numbers: 72.80.Vp, 73.22.Pr, 73.40.Gk, 78.67.Wj

Growing interest in graphene [1] is stimulated by many unusual and sometimes counterintuitive properties of this two-dimensional material. Indeed, graphene supplies charge carriers exhibiting pseudorelativistic dynamics of massless Dirac fermions. As one consequence, the Klein tunneling phenomenon [2] occurs with unit probability through arbitrarily high and thick barriers at perpendicular incidence, irrespective of the particle energy, in accordance with experiment [3]. The question of how to control the electron motion in graphene arose, and hence boosted detailed studies of Dirac fermions under the influence of various forms of scalar [4–8] or vector [9] potentials.

Applying a time-dependent laser field to pristine graphene opens an alternative and efficient way [10–12] to control spectrum and transport properties. It was shown [10] that Dirac fermions accross p-n junctions can acquire an effective mass when driven by a laser field. This results in an exponential suppression of chiral tunneling even for perpendicular incidence upon the junction, if the ac-electric field is directed parallel to the junction, in stark contrast to Klein tunneling occurring in the absence of the laser field. Actually, time-dependent laser fields can mimic [12] the influence of any electrostatic and/or magnetostatic graphene superlattice on the electron spectrum in graphene. The question arises whether and under which conditions time-dependent modulations of an electrostatic barrier, where energy is not conserved, would affect electron transport and generate backscattering.

In this Letter we answer this question by solving the problem for arbitrary space-time dependent scalar potentials $U(x, t)$. Our solution is based on expanding the wave function as a power series with respect to the momentum k_y parallel to the barrier, and manifests a structure of left and right moving waves. All terms appearing in the k_y expansion can be calculated analytically, despite the fact that each term is described by a partial differential equation in (x, t) space. At $k_y = 0$ (normal incidence upon the barrier) we confirm complete Klein tunneling for any $U(x, t)$, while for finite k_y backscattering resonances can occur at certain angles of incidence, depending on the modulation frequency of the barrier. As a counterintuitive result we find a nonzero and oscillating current j_y *along* the barrier, even at $k_y = 0$ for valley-polarized fermions. At $k_y \neq 0$ the current j_y arises also in valley-unpolarized situations, it can be resonantly amplified and flow in either direction. Interestingly, j_y exhibits a nonzero dc component at certain resonance frequencies, in full analogy to Shapiro steps of driven Josephson junctions.

At low energies, the honeycomb lattice of graphene engenders two copies, $\tau_z = \pm 1$, of Dirac-Weyl Hamiltonians [13],

$$H_0 = v_F[\hat{\tau}_z \hat{\sigma}_x \hat{p}_x + \hat{\sigma}_y \hat{p}_y], \tag{1}$$

centered about two inequivalent Dirac points ("valleys") K and K' at corners of the hexagonal first Brillouin zone where electron-hole symmetric bands touch; Pauli matrices $\hat{\sigma}_{x,y,z}$ act on two-component spinors representing sublattice amplitudes. Carriers near either of the Dirac points exhibit opposite Fermion helicities, $\boldsymbol{\sigma} \cdot \boldsymbol{p}/p = \pm 1$. Proposals exist in literature of how to valley polarize carriers in graphene, by means of nanoribbons terminated by zigzag edges [14], by exploiting trigonal warping at elevated energies [15], or by absorbing magnetic textures [16].

Smooth electromagnetic or disorder potentials [17], containing negligible Fourier components at large wave vectors of the order of $|\vec{K}|$, will not cause scattering between valleys so that calculations can be carried out for $\tau_z = +1$ or $\tau_z = -1$ separately. Accordingly, time-dependent potentials $U(x, t)$ should be slowly varying, without frequency components that might induce excursions to energies where the band structure of graphene starts deviating from the isotropic cone spectrum, i.e., below 0.6 eV [18]. Including $U(x, t)$, the Dirac equation for the wave function $\Psi_{k_y}(x, y, t) = \Psi(x, t) \exp(ik_y y)$ can be written in the form

$$\begin{pmatrix} U(x,t) & -i\tau_z \frac{\partial}{\partial x} \\ -i\tau_z \frac{\partial}{\partial x} & U(x,t) \end{pmatrix}\Psi + ik_y \begin{pmatrix} 0 & -1 \\ 1 & 0 \end{pmatrix}\Psi = i\frac{\partial}{\partial t}\Psi, \quad (2)$$

where from now on we assume $v_F = 1$ and $\hbar = 1$. This equation has been solved analytically for time-independent potentials either by matching [2] of wave functions for rectangular barriers or by the WKB method [19] for smooth barriers. Time-dependent harmonic oscillations have been considered of gate voltages on either side of a graphene rectangle [20], of an electric field parallel to the barrier [10] or in resonance approximation [12], or for some class of time-dependent barriers $U(x, t)$ at $k_y = 0$ [21].

Our goal here is to construct the solution of Eq. (2) for arbitrary $U(x, t)$ acting at positive times, $U(x, t < 0) = 0$. From the ansatz

$$\Psi = \sum_{n=0}^{\infty}(ik_y)^n \begin{pmatrix} 1 \\ \tau_z \end{pmatrix}\Psi_{n,+} + \sum_{n=0}^{\infty}(ik_y)^n \begin{pmatrix} 1 \\ -\tau_z \end{pmatrix}\Psi_{n,-} \quad (3)$$

as a power series in k_y we derive a recurrence relation for the coefficients $\Psi_{n,\pm}$ which obey the inhomogeneous first order partial differential equations,

$$\left[U(x,t) \mp i\frac{\partial}{\partial x} - i\frac{\partial}{\partial t}\right]\Psi_{n,\pm} \pm \tau_z\Psi_{n-1,\mp} = 0, \quad (4)$$

with $\Psi_{-1,\pm}(x, t \geq 0) \equiv 0$. Initial conditions can be chosen as $\Psi_{0,\pm}(x, t = 0) = a_\pm(x) = [\Psi_A(x, t = 0) \pm \tau_z\Psi_B(x, t = 0)]/2$, $\Psi_{n>0,\pm} = 0$, where Ψ_A, Ψ_B describe electron amplitudes on either of the graphene sublattices. The two functions $a_\pm(x)$, providing the initial conditions, can be, e.g., a plane wave or a wave packet. We underline here the general structure of (3) as a sum of right Ψ_+ and left Ψ_- moving waves. Using the standard d'Alembert's ratio test, a sufficient criterion for convergence of series (3) is $|k_y|\lim_{n\to\infty}|\Psi_{n+1,\pm}|/|\Psi_{n,\mp}| < 1$ for all relevant x and t.

Despite the fact that (4) are partial differential equations, we can solve them exactly using the method of characteristics [22]. The corresponding result reads

$$\Psi_{n,\pm}(x,t) = a_{n,\pm}(x,t)e^{-i\int_0^t dt' U(x\mp t\pm t',t')}, \quad (5)$$

with $a_{0,\pm} = a_\pm(x \mp t)$ and

$$a_{n>0,\pm} = \mp i\tau_z \int_0^t dt' \Psi_{n-1,\mp}(x \mp t \pm t', t') \times e^{i\int_0^{t'} dt'' U(x\mp t\pm t'',t'')}.$$

Together with (3) the recursive solution for $\Psi_{n,\pm}$ provides the exact wave function Ψ to any desired accuracy. To zeroth order approximation with respect to k_y, we obtain

$$\psi(x,t) = a_+(x-t)\begin{pmatrix} 1 \\ \tau_z \end{pmatrix} e^{-i\int_0^t dt' U(x-t+t',t')} + a_-(x+t)\begin{pmatrix} 1 \\ -\tau_z \end{pmatrix} e^{-i\int_0^t dt' U(x+t-t',t')}. \quad (6)$$

The first order corrections with respect to k_y in (5) can be written as

$$a_{1,\pm} = \mp i\tau_z A_{1,\pm} = \mp i\tau_z \int_0^t dt' a_\mp(x \mp t \pm 2t') \times e^{i\int_0^{t'} dt''[U(x\mp t\pm t'',t'') - U(x\mp t\pm 2t'\mp t'',t'')]}, \quad (7)$$

so that $\Psi = \Psi_+\binom{1}{\tau_z} + \Psi_-\binom{1}{-\tau_z}$ as in (3), with

$$\Psi_\pm = [a_{0,\pm} \pm k_y\tau_z A_{1\pm}]e^{-i\int_0^t dt' U(x\mp t\pm t',t')}. \quad (8)$$

When $k_y = 0$ and when the wave packet is initially purely right moving, $a_- = 0$, Eq. (6) reveals that the electron density distribution $|a_+(x - t)|^2$ undistortedly continues to propagate to the right without reflection: $\Psi_-(x, t) = 0$ for all times $t > 0$. This proves complete Klein tunneling also in the presence of time-dependent barriers; wave functions $\Psi_\pm$ acquire only a phase factor by the potential at $k_y = 0$.

As a measurable quantity, we now evaluate the current density in Cartesian components, $j_x = \Psi^*\tau_z\sigma_x\Psi = 2\Psi_+^*\Psi_+ - 2\Psi_-^*\Psi_- = j_{0x} + j_{1x}$ and $j_y = \Psi^*\sigma_y\Psi = 2i\tau_z(\Psi_+^*\Psi_- - \Psi_+\Psi_-^*) = j_{0y} + j_{1y}$. Here, the last equals signs refer to zeroth and first order contributions with respect to k_y, respectively, yielding

$$j_{0x} = 2(|a_{0+}|^2 - |a_{0-}|^2), \quad (9)$$

$$j_{0y} = 4\tau_z|a_{0+}a_{0-}|\sin(\varphi + \phi_0), \quad (10)$$

$$j_{1x} = 4k_y\tau_z\Re e\{a_{0+}A_{1+}^* - a_{0-}A_{1-}^*\}, \quad (11)$$

$$j_{1y} = 4k_y[|A_{1+}a_{0-}^*|\sin(\varphi - \phi_-) - |A_{1-}^*a_{0+}|\sin(\varphi + \phi_+)], \quad (12)$$

with $\varphi = \int_0^t[U(x + t - t', t') - U(x - t + t', t')]dt'$, $\phi_0 = \arg(a_{0+}a_{0-}^*)$, and $\phi_\pm = \arg(a_{0\pm}A_{1\mp}^*)$. We distinguish two cases: (i) τ_z-independent contributions j_{0x} and j_{1y} which can be observed for valley-unpolarized carriers and (ii) τ_z-dependent contributions j_{1x} and j_{0y} where detection calls for valley polarization.

Equations (9) and (10) describe the current density at normal incidence, $k_y = 0$. Then j_x stays unaffected by the barrier, irrespective of τ_z which rephrases the above result of complete Klein tunneling. Surprisingly, a current j_y flows perpendicular to the momentum in graphene, provided the sample is valley polarized [the total current $\boldsymbol{j} = \boldsymbol{j}^+ + \boldsymbol{j}^-$, where $\boldsymbol{j}^{\tau_z}$ originates from states near valley

K ($\tau_z = +1$) or K' ($\tau_z = -1$), respectively]. This current (10) results from interfering left and right moving waves, which both need to have nonzero amplitudes, $a_{0+}a_{0-} \neq 0$.

Equations (11) and (12) describe corrections to the current density at small but finite angles of incidence, $k_y \neq 0$. Thereby, j_{1x} exhibits qualitatively similar properties to j_{0y}; in particular, it stays nonvanishing at finite valley polarization only. By contrast, the current density j_{1y} now exhibits striking current oscillations and current reversals already in valley-unpolarized situations, as we show in more detail below.

Next we turn to the question of how carriers are reflected by $U(x, t)$. Let us consider an initially right moving plane wave, $\Psi_{k_y} = e^{i(k_x x + k_y y)}\binom{1}{\tau_z}$ at $t = 0$ which produces a current density $j_{0x} = +2$ pointing to the right. Using Eqs. (3) and (8), and assuming small k_y, the leading contribution to the reflected current density $j_{2x} = -k_y^2|A_{1-}|^2$ arises in $\mathcal{O}(k_y^2)$ under the action of the barrier at $t > 0$ and is proportional to $|j_{0x}|$, cf. Eqs. (7) and (9). This suggests to employ the ratio

$$R(x, t) := -j_{2x}/j_{0x} = k_y^2|A_{1-}(x, t)|^2/2 \qquad (13)$$

as a measure for the reflectivity at small k_y. While the quantity $R(x, t)$ evolves in time, together with $U(x, t)$, it is independent of τ_z and, thus, measurable without valley polarization. Moreover, we also analyze the time averaged reflectivity $\bar{R}(x) := \lim_{T\to\infty} \int_0^T R(x, t)dt/T$, which can be measured just by means of dc equipment.

In the following, two specific examples $U(x, t) = U^{(1,2)}(x, t)$ are considered. As initial conditions we take into account two cases: (i) a superposition of equal amplitudes of right and left propagating plane waves, $a_\pm = \exp(\pm i k_x x)$ and $\tau_z = +1$ when calculating j_{0y}, and (ii) an incidently right moving wave $a_+ = \exp(i k_x x)$, $a_- = 0$ when calculating R and j_{1y} for valley-unpolarized systems. Our first example is $U^{(1)}(x, t) = U_0 x \sin\omega t$. In view of (10), we derive for this case

$$j_{0y}(x, t) = \sin 2\left[k_x x + U_0\left(\frac{t}{\omega} - \frac{\sin\omega t}{\omega^2}\right)\right], \qquad (14)$$

which can be rewritten as a sum

$$j_{0y}(x, t) = \sum_{n=-\infty}^{\infty} J_n\left(\frac{2U_0}{\omega^2}\right)\sin\left(2k_x x + \frac{2U_0 t}{\omega} - n\omega t\right), \qquad (15)$$

using Bessel functions J_n. This form (15) reveals a peculiarity at $\omega = \omega_n$ with

$$\omega_n = \sqrt{2U_0/n}, \qquad n \in \mathbb{N}, \qquad (16)$$

similar to Shapiro steps [23] of a driven Josephson junction. As depicted in Fig. 1(a), frequencies $\omega = \omega_n$ generate periodic oscillations, which, again as in the case of

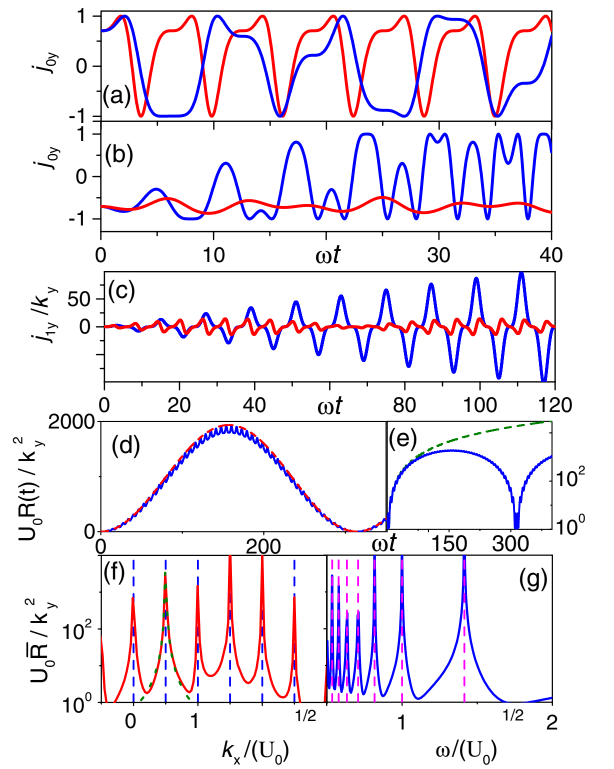

FIG. 1 (color online). (a) Current j_{0y} (10) perpendicular to $\boldsymbol{k}$ versus time for $U^{(1)}(x, t) = U_0 x \sin\omega t$, $k_x x = \pi/8$, and $U_0/\omega^2 = 1/\pi$ [dark gray (blue) line] and $U_0/\omega^2 = 1/2$ [light gray (red) line], assuming a valley-polarized situation $\tau_z = 1$. For "Shapiro-step" conditions [Eq. (16)] periodic oscillations can be seen [light gray (red)], while away from this condition aperiodic oscillations occur [dark gray (blue)]. (b) Same as (a) but for potential $U^{(2)}(x, t) = U_0\cos(x/L)\cos\omega t$ with $x = \pi L/2$, $k_x = 0$, $U_0 L = 0.1$, and frequencies $\omega = (\pi/2)(1/L)$ [light gray (red) line] and $\omega = 1/L$ [dark gray (blue) line]. Both currents are aperiodic. For the matching condition $\omega = 1/L$ [dark gray (blue)] a considerable enhancement followed by a saturation of the amplitude of the current oscillations occurs, while away from this resonance no enhancement is seen versus time. (c) Current j_{1y} (12) for $U^{(1)}(x, t)$ at $x = 0$, using $k_x = 0$. At Shapiro resonance [$U_0/\omega^2 = 1/2$, dark gray (blue) line] pronounced current enhancement occurs, cf. Eqs. (17) and (18), while away from the resonance [$U_0/\omega^2 = 3/\pi$, light gray (red) line] no enhancement is seen. (d) Time-dependent reflectivity $R(t)$, calculated by numerical integration of Eq. (17), solid blue line, and by using the approximation (19), red dashed line, near resonance for $k_x/\sqrt{U_0} = 0$ and $\omega^2/U_0 = 0.49$. (e) $R(t)$ at resonance (dashed green line, $k_x/\sqrt{U_0} = 0$, $\omega^2/U_0 = 1/2$) and near resonance (solid blue line, $k_x/\sqrt{U_0} = 0$, $\omega^2/U_0 = 0.49$). At the resonance, $R(t)$ increases with time $\sim t^2$, in agreement with Eq. (19). (f) Time-averaged reflectivity $\bar{R}$ as a function of $k_x/\sqrt{U_0}$ for $\omega/\sqrt{U_0} = 1$. Equidistant resonances occur at $k_x/\sqrt{U_0} = 1 - n/2$ (dashed blue vertical lines), cf. Eq. (18). One of the resonance peaks is well fitted by the resonance equation (20), as shown by short-dashed green line. (g) $\bar{R}$ as a function of the driving frequency $\omega/\sqrt{U_0}$ for $k_x/\sqrt{U_0} = 0$: resonance peaks are clearly seen at Shapiro-step conditions (18) $\omega/\sqrt{U_0} = \sqrt{2/n}$, indicated as dashed magenta vertical lines.

Shapiro steps, induce a nonzero dc component in the current at given x. Modulating the potential with $\omega \neq \omega_n$ results in aperiodic oscillations and zero dc component.

Similar resonance effects can also be seen in both the reflectivity R (13) and the current j_{1y} (12). By inserting $U^{(1)}(x, t)$ into Eq. (7), we derive

$$A_{1-} = e^{ik_x(x+t)} \int_0^t dt' e^{-2ik_x t'} e^{2iU_0[\omega t' - \sin(\omega t')]/\omega^2} = e^{ik_x(x+t)} \sum_{n=-\infty}^{\infty} J_n\left(\frac{2U_0}{\omega^2}\right) \frac{e^{i(2U_0/\omega - 2k_x - n\omega)t} - 1}{i(2U_0/\omega - 2k_x - n\omega)}, \quad (17)$$

from which we read off a Shapiro step resonance condition

$$k_n = k_x = -\frac{n}{2}\omega + \frac{U_0}{\omega}, \qquad n \in \mathbb{N} \quad (18)$$

specifying now a *directional* dependence of the momentum $\boldsymbol{k}$. From (17) together with (12) we conclude that in valley-unpolarized samples the current $j_y \propto k_y$ parallel to the barrier oscillates as a function of time and may take either sign [despite the fixed k_y, see Fig. 1(c)]. In addition, the amplitude of these oscillations increases with time as the Shapiro step resonance condition (18) is met [compare light gray (red) and dark gray (blue) curves in Fig. 1(c)].

Analogous resonances also show up in both reflectivities, R and $\bar{R}$. The latter allows experimental observation of the here predicted behavior without time-domain measurements. Indeed, near the Shapiro step resonance (18) we can keep only one summand in the expansion (17), yielding

$$R(t) = \frac{1}{2} k_y^2 J_n^2\left(\frac{2U_0}{\omega^2}\right) \frac{\sin^2[(U_0 - k_x - n\omega/2)t]}{(U_0/\omega - k_x - n\omega/2)^2}. \quad (19)$$

This equation is in a good agreement with numerical integration of (17); see Figs. 1(d) and 1(e). Averaging (19) with respect to time results in

$$\bar{R} = \frac{1}{4} k_y^2 J_n^2\left(\frac{2U_0}{\omega^2}\right) \frac{1}{(U_0/\omega - k_x - n\omega/2)^2}, \quad (20)$$

so that the barrier will become intransparent near momenta $k_x = k_n$ [see Fig. 1(f)], already for small U_0. This produces strong anomalies in transport properties at angles $\arctan(k_n/k_y)$ of the incidence. Instead of sweeping the directions of $\boldsymbol{k}$ one may alternatively sweep ω at fixed $\boldsymbol{k}$, cf. (18); ensuing resonance peaks are clearly observed in Fig. 1(g). The constraint $R < 1$ determines the maximum value

$$|k_y| \lesssim \frac{|U_0 - k_x - n\omega/2|}{|J_n(2U_0/\omega^2)|}, \quad (21)$$

where second and higher order terms in the expansion (3) can be ignored.

As a second example, we consider $U^{(2)}(x, t) = U_0 \cos(x/L) \cos\omega t$ to demonstrate how even more intriguing resonance features can arise from the interplay between spatial *and* temporal periodicities. Given again the initial condition of left and right moving plane waves of equal amplitudes, and assuming valley polarization, we find

$$j_{0y} = \sin\left\{2k_x x - \frac{4U_0 L \sin(\frac{x}{L})}{\omega^2 L^2 - 1} \sin\left[\frac{\omega L + 1}{2L} t\right] \sin\left[\frac{\omega L - 1}{2L} t\right]\right\}. \quad (22)$$

Now, oscillations of j_{0y} persist even when $\omega \to 0$, since the spatial periodicity $2\pi L$ of the potential induces a frequency component v_F/L to waves moving at the uniform Fermi velocity (restoring here v_F). This is reminiscent of the ac-Josephson effect [23] where ac-current oscillations are generated by a time-independent voltage.

On the other hand, if the barrier modulation frequency $\omega \to \pm v_F/L$, the argument of the sine in the curly brackets (22) varies proportional to t as $2k_x x \mp tU_0 \sin(x/L) \times \sin\omega t$. For small U_0 the oscillations of j_{0y} thus grow resonantly with time, before they saturate at $t \gtrsim 2\pi/U_0$, cf. Fig. 1(b). We mention the analogy to resonant excitations of plasmonic oscillations by spatiotemporal mode matching of the incident light with the grating period (Wood's anomaly [24]). Similar effects also occur for valley-unpolarized currents (e.g., j_{1y}) and the reflectivity $R(x, t)$, but calculations become considerably more cumbersome and will be published elsewhere.

In conclusion, we present the analytical solution of the Dirac equation for Fermions in graphene moving in a scalar potential barrier $U(x, t)$ of arbitrary x and time dependence. Unit transmission probability, referred to as Klein tunneling, is found for normal incidence upon the barrier, rendering at most a phase to the wave function. On the other hand, under certain angles with respect to the barrier ($k_y \neq 0$), we predict strong reflection, even for weak potentials. Further, also the current parallel to the barrier, j_y, may exhibit oscillations, despite a constant electron momentum k_y. The amplitude of these oscillations grows linearly in time when $U(x, t)$ meets certain resonance frequencies. In valley-polarized samples j_y does not vanish even for zero momentum parallel to the barrier ($k_y = 0$), provided left and right moving waves both interfere with finite amplitudes. For graphene nanostructures driven by oscillating potentials, the predicted resonances in current and reflectivity can be seen, for example, in electron transport properties (e.g., in ac and dc electrical conductivity) through suitably arranged quantum point contacts. The new nonstationary phenomena in graphene calculated here within the single-particle approximation can promote development of a more elaborate many-electron nonstationary theory of ac-driven graphene nanostructures which is crucial for future graphene-based electronics.

S. E. S. acknowledges support from the Alexander von Humboldt foundation through the Bessel prize and thanks Sasha Alexandrov and Viktor Kabanov for stimulating discussions. P. H. acknowledges support by the cluster of excellence, Nanosystems Initiative Munich (NIM).

[1] K. S. Novoselov, A. K. Geim, S. V. Morozov, D. Jiang, M. I. Katsnelson, I. V. Grigorieva, S. V. Dubonos, and A. A. Firsov, Nature (London) **438**, 197 (2005); A. H. C. Neto, N. M. R. Peres, K. S. Novoselov, and A. K. Geim, Rev. Mod. Phys. **81**, 109 (2009); A. V. Rozhkov, G. Giavaras, Y. P. Bliokh, V. Freilikher, and F. Nori, Phys. Rep. **503**, 77 (2011).
[2] M. I. Katsnelson, K. S. Novoselov, and A. K. Geim, Nat. Phys. **2**, 620 (2006).
[3] N. Stander, B. Huard, and D. Goldhaber-Gordon, Phys. Rev. Lett. **102**, 026807 (2009); A. F. Young and P. Kim, Nat. Phys. **5**, 222 (2009); S.-G. Nam, D.-K. Ki, J. W. Park, Y. Kim, J. S. Kim, and H.-J. Lee, Nanotechnology **22**, 415 203 (2011).
[4] C. X. Bai and X. D. Zhang, Phys. Rev. B **76**, 075430 (2007); C. H. Park, L. Yang, Y.-W. Son, M. L. Cohen, and S. G. Louie, Nat. Phys. **4**, 213 (2008); C. H. Park, L. Yang, Y.-W. Son, M. Cohen, and S. Louie, Phys. Rev. Lett. **101**, 126804 (2008); M. Barbier, P. Vasilopoulos, and F. M. Peeters, Phys. Rev. B **81**, 075438 (2010); L. Z. Tan, C. H. Park, and S. G. Louie, Phys. Rev. B **81**, 195426 (2010).
[5] Y. P. Bliokh, V. Freilikher, S. Savel'ev, and F. Nori, Phys. Rev. B **79**, 075123 (2009).
[6] V. V. Cheianov, V. I. Fal'ko, and B. L. Altshuler, Science **315**, 1252 (2007); V. A. Yampol'skii, S. Savel'ev, and F. Nori, New J. Phys. **10**, 053024 (2008).
[7] M. Barbier, P. Vasilopoulos, and F. M. Peeters, Phys. Rev. B **80**, 205415 (2009).
[8] H.-Y. Chiu, V. Perebeinos, Y.-M. Lin, and P. Avouris, Nano Lett. **10**, 4634 (2010); M. Y. Han, B. Özyilmaz, Y. Zhang, and P. Kim, Phys. Rev. Lett. **98**, 206805 (2007); B. Huard, J. Sulpizio, N. Stander, K. Todd, B. Yang, and D. Goldhaber-Gordon, Phys. Rev. Lett. **98**, 236803 (2007).
[9] T. K. Ghosh, A. De Martino, W. Häusler, L. Dell'Anna, and R. Egger, Phys. Rev. B **77**, 081404 (2008); W. Häusler, A. De Martino, T. Ghosh, and R. Egger, Phys. Rev. B **78**, 165402 (2008); W. Häusler and R. Egger, Phys. Rev. B **80**, 161402(R) (2009).
[10] M. V. Fistul and K. B. Efetov, Phys. Rev. Lett. **98**, 256803 (2007).
[11] H. L. Calvo, H. M. Pastawski, S. Roche, and L. E. F. F. Torres, Appl. Phys. Lett. **98**, 232 103 (2011).
[12] S. E. Savel'ev and A. S. Alexandrov, Phys. Rev. B **84**, 035428 (2011).
[13] C. L. Kane and E. J. Mele, Phys. Rev. Lett. **95**, 226801 (2005).
[14] A. Rycerz, J. Tworzydlo, and C. W. J. Beenakker, Nat. Phys. **3**, 172 (2007); A. R. Akhmerov, J. Bardarson, A. Rycerz, and C. Beenakker, Phys. Rev. B **77**, 205416 (2008); J. M. Pereira, Jr., F. M. Peeters, R. N. C. Filho, and G. A. Farias, J. Phys. Condens. Matter **21**, 045301 (2009).
[15] J. L. Garcia-Pomar, A. Cortijo, and M. Nieto-Vesperinas, Phys. Rev. Lett. **100**, 236801 (2008).
[16] A. Hill, A. Sinner, and K. Ziegler, New J. Phys. **13**, 035023 (2011).
[17] T. Ando, T. Nakanishi, and R. Saito, J. Phys. Soc. Jpn. **67**, 2857 (1998).
[18] S. Y. Zhou, G.-H. Gweon, J. Graf, A. V. Fedorov, C. D. Spataru, R. D. Diehl, Y. Kopelevich, D.-H. Lee, S. G. Louie, and A. Lanzara, Nat. Phys. **2**, 595 (2006).
[19] V. V. Cheianov and V. I. Fal'ko, Phys. Rev. B **74**, 041403 (R) (2006); P. G. Silvestrov and K. B. Efetov, Phys. Rev. Lett. **98**, 016802 (2007); S. V. Syzranov, M. V. Fistul, and K. B. Efetov, Phys. Rev. B **78**, 045407 (2008).
[20] B. Trauzettel, Ya. M. Blanter, and A. F. Morpurgo, Phys. Rev. B **75**, 035305 (2007); P. San-Jose, E. Prada, H. Schomerus, and S. Kohler Appl. Phys. Lett. **101**, 153506 (2012).
[21] D. Solomon, Can. J. Phys. **88**, 137 (2010).
[22] R. Courant, D. Hilbert, *Methods of Mathematical Physics* (Wiley-Interscience, New York, 1962), Vol. 2.
[23] M. Tinkham, *Introduction to Superconductivity* (Dover, New York, 2004).
[24] H. Raether, *Surface Plasmons* (Springer, New York, 1988).